Applied Surface Science 396 (2017) 221–225

Contents lists available at ScienceDirect

Applied Surface Science

journal homepage: www.elsevier.com/locate/apsusc

Full Length Article

Narrow titanium oxide nanowires induced by femtosecond laser pulses on a titanium surface

Hui Li[a], Xian-Feng Li[a], Cheng-Yun Zhang[b], Shao-Long Tie[c], Sheng Lan[a,*]

[a] Laboratory of Nanophotonic Functional Materials and Devices, School of Information and Optoelectronic Science and Engineering, South China Normal University, Guangzhou 510006, China
[b] School of Physics and Electronic Engineering, Guangzhou University, Guangzhou 510006, China
[c] School of Chemistry and Environment, South China Normal University, Guangzhou 510006, China

ARTICLE INFO

Article history:
Received 12 April 2016
Received in revised form 2 October 2016
Accepted 14 October 2016
Available online 18 October 2016

Keywords:
Nanostructure fabrication
Laser materials processing
Subwavelength structures
Nanostructures

ABSTRACT

The evolution of the nanostructure induced on a titanium (Ti) surface with increasing irradiation pulse number by using a 400-nm femtosecond laser was examined by using scanning electron microscopy. High spatial frequency periodic structures of TiO_2 parallel to the laser polarization were initially observed because of the laser-induced oxidation of the Ti surface and the larger efficacy factor of TiO_2 in this direction. Periodically aligned TiO_2 nanowires with featured width as small as 20 nm were obtained. With increasing pulse number, however, low spatial frequency periodic structures of Ti perpendicular to the laser polarization became dominant because Ti possesses a larger efficacy factor in this direction. The competition between the high- and low-spatial frequency periodic structures is in good agreement with the prediction of the efficacy factor theory and it should also be observed in the femtosecond laser ablation of other metals which are easily oxidized in air.

1. Introduction

Femtosecond (fs) laser ablation has attracted great interest in the last two decades because of its capability in the fabrication of micro- and nanostructures (including micro- and nanoparticles) [1–3]. In recent years, the laser-induced periodic surface structures (LIPSSs) on the surfaces of different materials by using laser fluence near the ablation threshold have become the focus of many studies [4–13]. Apart from the conventional low spatial frequency LIPSSs (LSFLs) perpendicular to the laser polarization, much attention has been paid to the high spatial frequency LIPSSs (HSFLs) parallel to the laser polarization and HSFLs with sub-100-nm periods have been achieved [14,15].

So far, the most popular physical model used to interpret the formation of LIPSSs is the efficacy factor theory proposed more than thirty years ago by Sipe et al. [16]. It is based on the interference between the incident light and the scattered light [16,17]. Apart from the efficacy factor theory, different mechanisms have been proposed to explain the formation of HSFLs, such as self-organization [18], second harmonic generation [19–21], excitation of surface plasmon polaritons [22], and Coulomb explosion [23] etc. However, the actual physical mechanism responsible for the appearance of HSFLs is still debated. We also proposed a physical mechanism for the formation of HSFLs on metals based on the electric field redistribution induced by the initially formed LSFLs and it successfully explained the HSFLs induced on some metals [24]. For metals which are easily oxidized in air, the highly efficient nonlinear optical response of the oxides may play a crucial role in the formation of HSFLs [25]. So far, the ratio of ridge width to period in most HSFLs is generally larger than 0.50 and HSFLs are usually referred to as ripples. There is no report for the formation of nanowires with narrow widths.

Titanium (Ti) is a metal which has been widely applied in industry. LIPSSs created on the surface of Ti may significantly alter the physical properties of Ti, leading to some new functions [26]. Both LSFLs and HSFLs were observed in the fs laser ablation of Ti [27–29]. In particular, the shortest period of HSFLs was found to be only one-tenth of the irradiation laser wavelength and the physical mechanism responsible for the deep subwavelength period is still under investigation [28–33]. On the other hand, Ti is easily oxidized in air when it is heated to a high temperature, forming titanium oxide Ti_xO_y (such as TiO_2, Ti_2O_3, TiO, and TiO_{2-x}) [28,29,34]. In fact, sub-100-nm HSFLs have been demonstrated in the ablation of Ti by using fs laser pulses and it was suggested that laser-induced oxide (i.e., the formation of TiO_2 on the surface of Ti) might play an important role in the formation of such HSFLs [25,28].

* Corresponding author.
E-mail address: slan@scnu.edu.cn (S. Lan).

http://dx.doi.org/10.1016/j.apsusc.2016.10.075
0169-4332/

In this article, we investigate the evolution of the nanostructures induced on a titanium (Ti) surface with increasing number of femtosecond (fs) laser pulses for laser fluence near the ablation threshold. The ablation wavelength was chosen to be 400 nm at which there is perceivable absorption in titanium dioxide (TiO_2). It is found that TiO_2 nanowire arrays with a width as narrow as ~20 nm and a period as small as ~60 nm were obtained with the irradiation of a few pulses. With increasing pulse number, an increase of the period up to ~110 nm was observed. For pulse numbers larger than 10, LSFLs with a period close to the laser wavelength became dominant. An evolution of the surface structure from a HSFL to a LSFL with increasing pulse number was demonstrated. It can be qualitatively interpreted by the efficacy factor theory.

2. Experimental

In our experiment, the LIPSSs were produced on the surface of a 0.5-mm-thick Ti foil (MTI, China) by irradiating fs laser pulses at a wavelength (λ) of 400 nm which was obtained by doubling the frequency of a fs laser amplifier (Legend, Coherent) with a BBO crystal. The duration and repetition rate of the laser pulses were 100 fs and 1 kHz, respectively. The Ti foil was polycrystalline material with purity of 99% and surface roughness less than 5 nm. The laser beam with a diameter of ~5.1 mm and a Gaussian profile was focused normally on the surface of the Ti foil by using a lens with a focusing length of 150 mm, producing an excitation spot of ~40 μm in diameter (full width at $1/e^2$ of the laser intensity). The laser fluence (F), which is defined as the energy of a single pulse divided by the area of the excitation spot, was adjusted by using the combination of a waveplate and a polarizer. It was fixed at 95.5 mJ/cm^2 which is just above the ablation threshold of Ti after considering surface oxidation. With this laser fluence, the thin TiO_2 layer can be ablated with the help of Ti which also absorbs laser energy and contributes to the temperature rise. After the formation of the TiO_2 nanowires, the laser fluence is large enough to ablate the exposed Ti surface. The ablation was carried out in air by irradiating the surface of the Ti foil with different numbers of pulses (N) and we fired laser shots manually without a specific time between each pulse. The morphology of the ablated surface was examined by using scanning electron microscopy (SEM) (Ultra55, Zeiss). The composition of the formed nanostructures was characterized by the energy dispersive X-ray spectroscopy (EDX).

3. Results and discussion

3.1. Morphology of nanostructures induced by using different pulse numbers

The SEM images of the nanostructures induced on the Ti surface with increasing pulse number are presented in Fig. 1. The laser light was vertically polarized and its fluence was chosen to be F = 95.5 mJ/cm^2. For N = 3, one can see the appearance of a HSFL with a period of ~60 nm although it is vague. The morphology of the HSFL becomes clear for N = 5 at which one can see nanowires with a width as narrow as ~20 nm. The period of the nanowire array is estimated to be ~90 nm which is much larger than the width of the nanowires. This unique feature makes the HSFL clearly distinct from those observed previously [28,29,35–37]. The nanowires are aligned along the polarization of the laser. For N = 8, a LSFL perpendicular to the laser polarization emerges at the subsurface, as shown in Fig. 1(f). The LSFL appears to be clearer for N = 10 and becomes dominant for N = 15 [see Fig. 1(h)].

To estimate the periods of the LIPSSs, the SEM images are Fourier transformed and the one-dimensional results along the directions

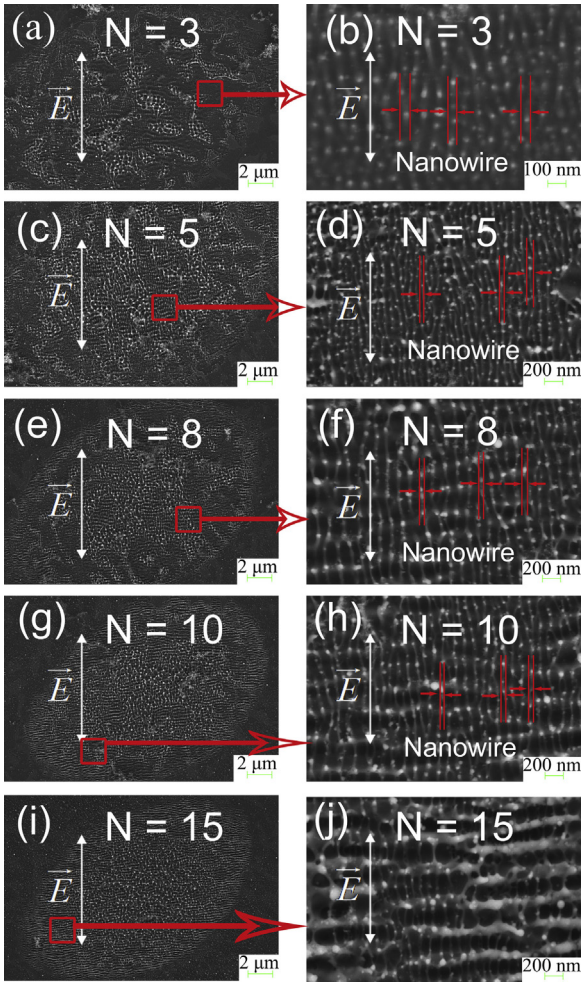

Fig. 1. Evolution of the nanostructure induced on the Ti surface with increasing pulse number. (a) and (b): N = 3, (c) and (d): N = 5, (e) and (f): N = 8, (g) and (h): N = 10, (i) and (j): N = 15. The laser light was vertically polarized and its fluence was fixed at F = 95.5 mJ/cm^2. The TiO_2 nanowires are indicated by two red vertical lines in (b), (d), (f), and (h). (For interpretation of the references to colour in this figure legend, the reader is referred to the web version of this article.)

parallel and perpendicular to the laser polarization are shown in Fig. 2. The two-dimensional results are also provided as insets. In the direction parallel to the laser polarization, one can see an increase of the period from ~60 to ~110 nm with increasing pulse number (see the left column of Fig. 2). The smallest period of ~60 nm is observed for N = 3. The maximum intensity of the Fourier transformation increases initially when N is increased from 3 to 5 and then decreases when N is further increased from 5 to 15. For N = 3, the morphology of the nanowires is not clear because of the small number of laser pulses. With increasing pulse number, the nanoridges get deeper, leading to the increase in the maximum intensity. For N = 8, the LSFLs beneath the nanowire array appear, leading to the decrease of the maximum intensity from the HSFLs. In addition, it is noticed that a peak corresponding to a period of ~227.3 nm emerges in the Fourier transformation along the direction perpendicular to the laser polarization, as shown in Fig. 2(f). For N = 15, a strong peak is observed at a wavevector of 3.2 μm^{-1}, corresponding to a period of ~312.5 nm which is close to the incident wavelength. In addition, the weakened peak in the direction parallel to the laser polarization indicates clearly that the surface is dominated by the LSFL.

As mentioned in Section 2, we used a lens with a long focal length of ~150 mm, which resulted in a laser spot with a diam-

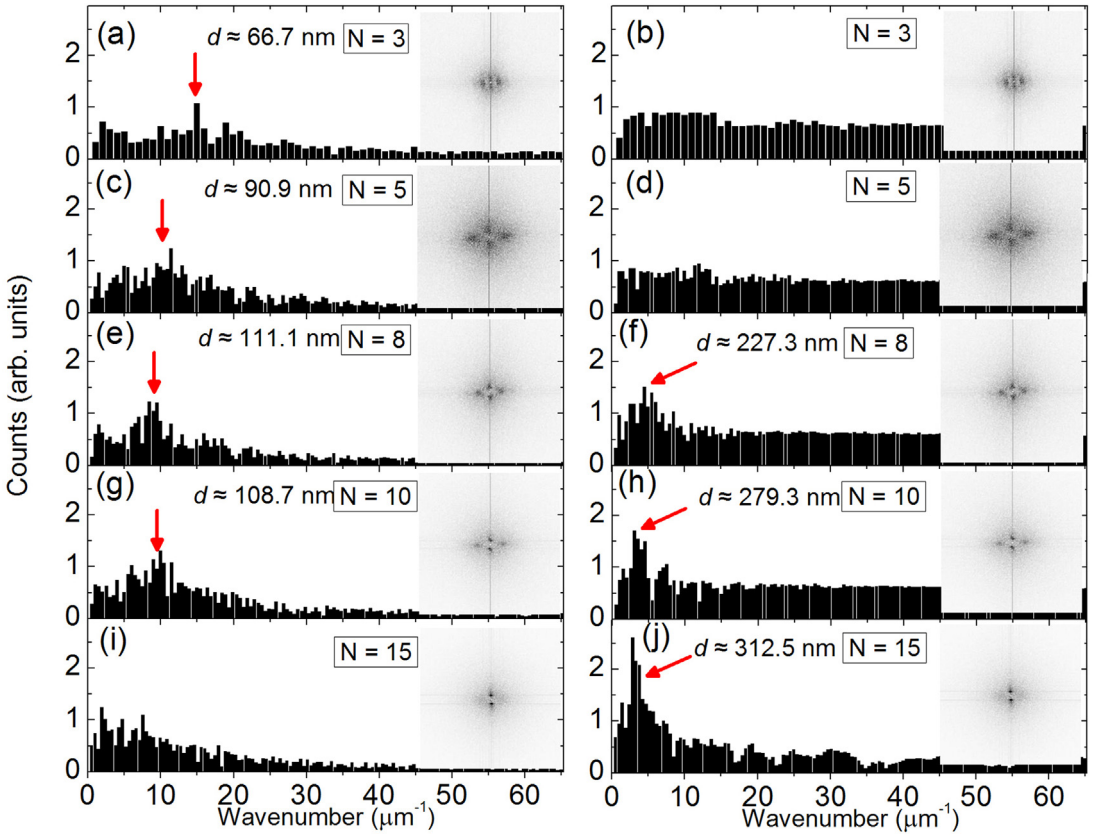

Fig. 2. One-dimensional Fourier transformations of the SEM images for the nanostructures along the directions parallel (left column) and perpendicular (right column) to the laser polarization. The two-dimensional Fourier transformations of the SEM images for the nanostructures are provided as insets.

eter of ~40 μm, to focus the laser light. Though the ablation area is larger than the laser spot, the SEM images show that there is little variation in the morphology across the ablation area. It may be noted that the debris caused by the ejected nanoparticles makes it difficult to compare the morphology at every location for different irradiation pulse numbers.

3.2. Composition of nanowires analyzed by EDX measurements

We employed EDX to examine the composition of the formed LIPSSs (HSFLs and LSFLs). The EDX measurements were carried out at an acceleration voltage of 15 kV on the nanowires induced by different iradiation pulse rnumbers, as shown in Fig. 3. The unablated area was also measured for comparison. Although the energy difference between the K_α and L_α peaks of Ti and oxygen (O) is only 72.7 eV, the content of O can be detected in the EDX spectra. Only C and Ti were found in the EDX spectrum of the unablated area. In general, a natural TiO_2 film is present on the surface of Ti because it can adsorb oxygen in ambient atmosphere. However, such a TiO_2 layer is too thin to be detected in the EDX measurement, as shown in Fig. 3(a). In comparison, the oxidation of the Ti surface becomes significant at high temperatures caused by the irradiation of fs laser pulses [see Fig. 3(b)–(d)]. As expected, an appreciable amount of O was detected in the LIPSSs and its content increases with increasing pulse number. The content of O (%) as a function of the irradiation pulses number is shown in Fig. 3(e). The O content measured for the nanowires could be an overestimate as the diameter of the electron beam (~30 nm) was larger than the width of the nanowires and also the penetration depth of the 15 keV electron beam was much larger than the height of the nanowires. However, the observation of O in the nanowires indicates clearly the formation of a thin Ti_xO_y film on the surface of the Ti foil. Since this work does not focus on the accurate determination of the nanowire composition, we did not perform other experiments such as Auger electron spectroscopy for this purpose. In the EDX measurements, carbon is generally detected because of the adsorbed carbon at the imaging site due to the high-energy electrons [38], as shown in Fig. 3. To characterize the crystallinity of the TiO_2 nanowires, one needs to carry out either transmission electron microscopy or X-ray diffraction measurement on the nanowires.

3.3. Explanation of the induced nanostructures based on the efficacy factor theory

In previous studies, the efficacy factor theory has been employed to analyze the morphology of LIPSSs, including their periods and orientations [16,17,28]. In order to understand the formation of TiO_2 nanowires, which belongs to a HSFL, and the simultaneous appearance of the HSFL and LSFL with increasing irradiation pulse number, we have examined the dependence of the efficacy factor (η) on the normalized wavevector ($k = \lambda/\Lambda$) for the nanostructures induced on the surfaces of Ti and TiO_2 when the laser wavelength is chosen to be $\lambda = 400$ nm, as shown in Fig. 4(a) and Fig. 4(b), respectively. Here, Λ is the period of the induced nanostructure. In the calculation, the complex refractive indices of Ti and TiO_2 were chosen to be 1.55 + 2.15i and 2.8181 + 0.0057i [39] while the shape and filling factors were chosen to be $s = 0.4$ and $f = 0.1$.

From the dependence of the efficacy factor on the normalized wavevector shown in Fig. 4(a) and Fig. 4(b), it is noticed that the maximum efficacy factor for the nanostructures on the surface of Ti appears in the κ_x direction while that for the nanostructures on the surface of TiO_2 appears in the κ_y direction. In addition, the former is achieved at $\kappa_x \sim 1.0$ while the latter is achieved at $\kappa_y \sim 2.7$, as can be seen in Fig. 4(c) and Fig. 4(d). Since κ_x is parallel to the laser

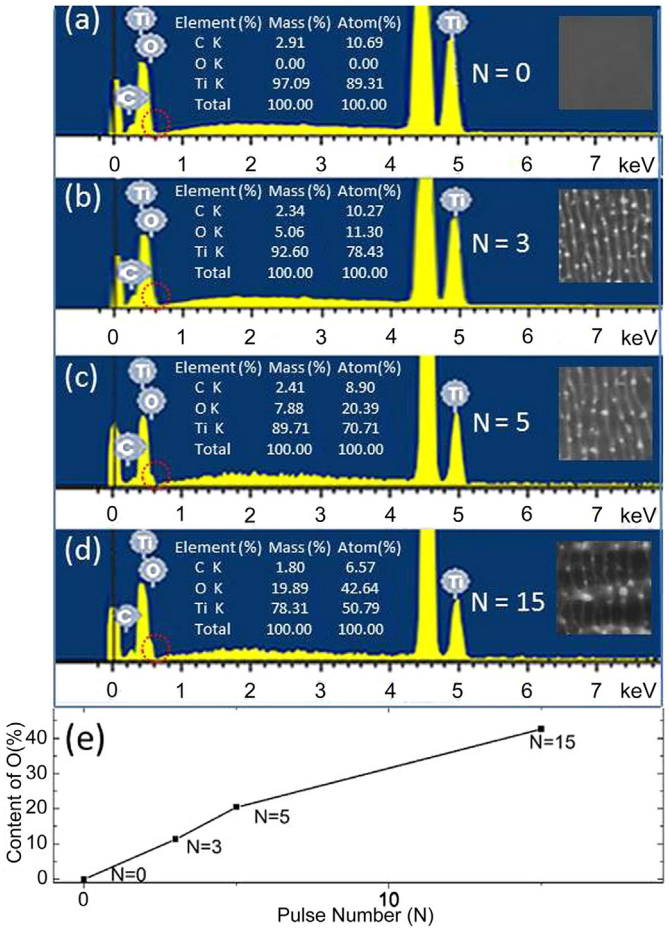

Fig. 3. EDX spectra measured for the unablated Ti surface (a) and the HSFLs induced by using different pulse numbers (b–d). The analysis of the elements and the corresponding SEM images are provided as insets. The content of O (%) versus the number of irradiation pulses is plotted in (e).

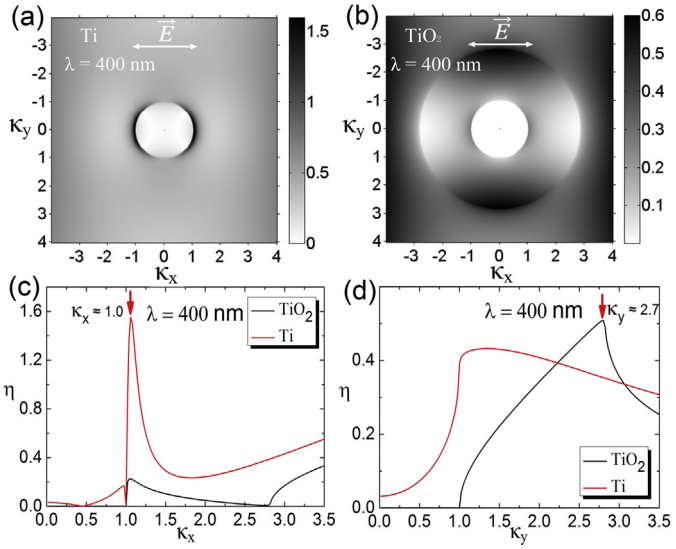

Fig. 4. Dependence of the efficacy factor η on the normalized wavevector **κ** (κ_x and κ_y) calculated at λ = 400 nm for the nanostructures induced on the surfaces of Ti (a) and TiO_2 (b) based on the efficacy factor theory. Comparison of the efficacy factor η for the nanostructures induced on the surfaces of Ti and TiO_2 along the κ_x (c) and κ_y (d) directions.

polarization and perpendicular to the orientation of the LIPSSs, it implies that LSFLs with periods approximately equal to the laser wavelength (i.e. $\kappa_x \sim 1.0$ or $\Lambda \sim \lambda$) and orientations perpendicular to the laser polarization are preferentially formed on the surface of Ti. In contrast, it is expected that HSFLs with periods much smaller than the laser wavelength (i.e. $\kappa_y \sim 2.7$ or $\Lambda \sim \lambda/2.7$) and orientations parallel to the laser polarization are preferentially formed on the surface of TiO_2.

As mentioned above, a natural TiO_2 layer is generally present on the surface of Ti although it is very thin. In the initial stage of the laser ablation, the energy of the fs laser pulses is absorbed mainly by Ti through both linear and nonlinear absorption. The rapid increase of the surface temperature leads to the further oxidation of the surface and the increase in the thickness of the thin TiO_2 layer. Although the linear absorption TiO_2 is negligible at 400 nm [39–41], the energy of the fs laser pulses can be absorbed by the thin TiO_2 layer through multi-photon-induced absorption. Meanwhile, the energy absorbed by Ti beneath the TiO_2 layer also results in the temperature rise in the TiO_2 layer. As discussed above, HSFLs with periods much smaller than the laser wavelength (i.e. $\kappa_y \sim 2.7$ or $\Lambda \sim \lambda/2.7$) and orientations parallel to the laser polarization are preferentially formed on the surface of TiO_2. Therefore, the formation of TiO_2 nanowire arrays, which belong to HSFLs, is observed for small pulse numbers (e.g. N = 3 and N = 5).

From Fig. 4(c) and Fig. 4(d), it can be seen that the maximum efficacy factor for the LSFL on the surface of Ti (~1.6) is much larger than that for the HSFL on the surface of TiO_2 (~0.5). After the formation of TiO_2 nanowires, the surface becomes dominated by Ti rather than TiO_2 because the width of the nanowires (~20 nm) is much smaller than the period of the nanowire array (~100 nm). Therefore, the ablation of the Ti surface becomes dominant, leading to the formation of the LSFLs perpendicular to the laser polarization. The competition between the HSFL and the LSFL observed in the experiments confirms the validity of the efficacy factor theory proposed more than thirty years ago [4]. By controlling the irradiation pulse number, one can selectively decorate the surface with HSFLs or LSFLs composed of nanostructures with different periods and orientations, implying potential applications in data storage, lithography and information encryption.

4. Conclusion

We have investigated the ablation of Ti surface by using 400-nm fs laser pulses and observed the evolution of the surface structure from a HSFL to a LSFL with increasing irradiation pulse number which verifies the validity of the efficacy factor theory. In addition, TiO_2 nanowires with a featured width as narrow as 20 nm were achieved by using pulse numbers smaller than 10. The physical mechanism for the formation of narrow nanowires will be effective for other metals which are easily oxidized in air. The dependence of the formed periodic nanostructures on the irradiation pulse number may find potential applications in the fields of data storage, lithography and information encryption.

Acknowledgments

Authors acknowledge the financial support from the National Natural Science Foundation of China (Grant Nos. 11374109 and 11674110), the Natural Science Foundation of Guangdong Province, China (Grant. No. 2016A030308010), and the Science and Technology Planning Project of Guangdong Province, China (Grant No. 2015B090927006).

References

[1] A.Y. Vorobyev, C. Guo, Femtosecond laser nanostructuring of metals, Opt. Express 14 (2006) 2164–2169.
[2] A.Y. Vorobyev, C. Guo, Colorizing metals with femtosecond laser pulses, Appl. Phys. Lett. 92 (2008) 041914.
[3] T.Y. Hwang, C. Guo, Polarization and angular effects of femtosecond laser-induced conical microstructures on Ni, J. Appl. Phys. 111 (2012) 083518.
[4] M. Ardron, N. Weston, D. Hand, A practical technique for the generation of highly uniform LIPSS, Appl. Surf. Sci. 313 (2014) 123–131.
[5] C.Y. Zhang, J.W. Yao, C.Q. Li, Q.F. Dai, S. Lan, V.A. Trofimov, T.M. Lysak, Asymmetric femtosecond laser ablation of silicon surface governed by the evolution of surface nanostructures, Opt. Express 21 (2013) 4439–4446.
[6] Y. Liu, Y. Brelet, Z. He, L. Yu, S. Mitryukovskiy, A. Houard, B. Forestier, A. Couairon, A. Mysyrowicz, Ciliary white light: optical aspect of ultrashort laser ablation on transparent dielectrics, Phys. Rev. Lett. 110 (2013) 097601.
[7] J. Reif, C. Martensa, S. Uhliga, M. Ratzke, O. Varlamova, S. Valette, S. Benayoun, On large area LIPSS coverage by multiple pulses, Appl. Surf. Sci. 336 (2015) 249–254.
[8] P. Slepička, O. Neděla, P. Sajdl, Z. Kolská, V. Švorčík, Polyethylene naphthalate as an excellent candidate for ripple nanopatterning, Appl. Surf. Sci. 285 (2013) 885–892.
[9] Q. Pang, D. Kundu, M. Cuisinier, L.F. Nazar, Surface-enhanced redox chemistry of polysulphides on a metallic and polar host for lithium-sulphur batteries, Nat. Commun. 5 (2014).
[10] E. Rebollar, J.R. Aldana, J. Pérez-Hernández, T. Ezquerra, P. Moreno, Ultraviolet and infrared femtosecond laser induced periodic surface structures on thin polymer films, Appl. Phys. Lett. 100 (2012) 041106.
[11] R.L. Harzic, D. Dörr, D. Sauer, M. Neumeier, M. Epple, H. Zimmermann, F. Stracke1, Large-area, uniform, high-spatial-frequency ripples generated on silicon using a nanojoule-femtosecond laser at high repetition rate, Opt. Lett. 36. 2 (2011) 229-231.
[12] R.L. Harzic, F. Stracke, H. Zimmermann, Formation mechanism of femtosecond laser-induced high spatial frequency ripples on semiconductors at low fluence and high repetition rate, J. Appl. Phys. 113 (2013) 183503.
[13] R.L. Harzic, H. Schuck, D. Sauer, T. Anhut, I. Riemann, K. König, Sub-100 nm nanostructuring of silicon by ultrashort laser pulses, Opt. Express 13 (2005) 6651–6656.
[14] J. Bonse, S. Höhmb, R. Koter, M. Hartelta, D. Spaltmann, S. Pentzien, A. Rosenfeld, J. Krüger, Tribological performance of sub-100-nm femtosecond laser-induced periodic surface structures on titanium, Appl. Surf. Sci. 374 (2016) 190–196.
[15] X. Sedao, M.V. Shugaev, C. Wu, T. Douillard, C. Esnouf, C. Maurice, S. Reynaud, F. Pigeon, F. Garrelie, L.V. Zhigilei, J. Colombier, Growth twinning and generation of high-frequency surface nanostructures in ultrafast laser-induced transient melting and resolidification, ACS Nano 10 (2016) 6995–7007.
[16] J.E. Sipe, J.F. Young, J.S. Preston, H.M. van Driel, Laser-induced periodic surface structure. I. Theory, Phys. Rev. B 27 (1983) 1141–1154.
[17] D. Dufft, A. Rosenfeld, S.K. Das, R. Grunwald, J. Bonse, Femtosecond laser-induced periodic surface structures revisited: a comparative study on ZnO, J. Appl. Phys. 105 (2009) 034908.
[18] F. Costache, M. Henyk, J. Reif, Modification of dielectric surfaces with ultra-short laser pulses, Appl. Surf. Sci. 186 (2002) 352–357.
[19] A. Borowiec, H.K. Haugen, Subwavelength ripple formation on the surfaces of compound semiconductors irradiated with femtosecond laser pulses, Appl. Phys. Lett. 82 (2003) 4462–4464.
[20] T.Q. Jia, H.X. Chen, M. Huang, F.L. Zhao, J.R. Qiu, R.X. Li, Z.Z. Xu, X.K. He, J. Zhang, H. Kuroda, Formation of nanogratings on the surface of a ZnSe crystal irradiated by femtosecond laser pulses, Phys. Rev. B 72 (2005) 125429.
[21] R.L. Harzic, D. Dörr, D. Sauer, F. Stracke, H. Zimmermann, Generation of high spatial frequency ripples on silicon under ultrashort laser pulses irradiation, Appl. Phys. Lett. 98 (2011) 211905.
[22] G. Miyaji, K. Miyazaki, Origin of periodicity in nanostructuring on thin film surfaces ablated with femtosecond laser pulses, Opt. Express 16 (2008) 16265–16271.
[23] Y. Dong, P. Molian, Coulomb explosion-induced formation of highly oriented nanoparticles on thin films of 3C–SiC by the femtosecond pulsed laser, Appl. Phys. Lett. 84 (2004) 10–12.
[24] J.W. Yao, C.Y. Zhang, H.Y. Liu, Q.F. Dai, L.J. Wu, S. Lan, A.V. Gopal, V.A. Trofimov, T.M. Lysak, High spatial frequency periodic structures induced on metal surface by femtosecond laser pulses, Opt. Express 20 (2012) 905–911.
[25] X.F. Li, C.Y. Zhang, H. Li, Q.F. Dai, S. Lan, S.L. Tie, Formation of 100-nm periodic structures on a titanium surface by exploiting the oxidation and third harmonic generation induced by femtosecond laser pulses, Opt. Express 22 (2014) 28086–28099.
[26] A.Y. Vorobyev, A.N. Topkov, O.V. Gurin, V.A. Svich, C.L. Guo, Enhanced absorption of metals over ultrabroad electromagnetic spectrum, Appl. Phys. Lett. 95 (2009) 121106.
[27] J. Wang, C. Guo, Formation of extraordinarily uniform periodic structures on metals induced by femtosecond laser pulses, J. Appl. Phys. 100 (2006) 023511.
[28] J. Bonse, S. Höhm, A. Rosenfeld, J. Krüger, Sub-100-nm laser-induced periodic surface structures upon irradiation of titanium by Ti: sapphire femtosecond laser pulses in air, Appl. Phys. A 110 (2013) 547–551.
[29] J. Bonse, J. Krüger, S. Höhm, A. Rosenfeld, Femtosecond laser-induced periodic surface structures, J. Laser Appl. 24 (2012) 042006.
[30] S.K. Das, A. Rosenfeld, M. Bock, A. Pfuch, W. Seeber, R. Grunwald, Scattering-controlled femtosecondlaser induced nanostructuring of TiO_2 thin films, Proc. SPIE 7925 (2011) 79251B.
[31] S.K. Das, C. Schwanke, A. Pfuch, W. Seeber, M. Bock, G. Steinmeyer, T. Elsaesser, R. Grunwald, Highly efficient THG in TiO_2 nanolayers for third-order pulse characterization, Opt. Express 19 (2011) 16985–16995.
[32] A. Borowiec, H.K. Haugen, Subwavelength ripple formation on the surfaces of compound semiconductors irradiated with femtosecond laser pulses, Appl. Phys. Lett. 82 (2003) 4462–4464.
[33] A.A. Ionin, S.I. Kudryashov, S.V. Makarov, L.V. Seleznev, D.V. Sinitsyn, A.E. Ligachev, E.V. Golosov, Yu R. Kolobov, Sub-100 nanometer transverse gratings written by femtosecond laser pulses on a titanium surface, Laser Phys. Lett. 10 (2013) 056004.
[34] J. Bonse, H. Sturm, D. Schmidt, W. Kautek, Chemical, morphological and accumulation phenomena in ultrashort-pulse laser ablation of TiN in air, Appl. Phys. A 71 (2000) 657–665.
[35] L. Gemini, M. Hashida, Y. Miyasaka, S. Inoue, J. Limpouch, T. Mocek, S. Sakabe, Periodic surface structures on titanium self-organized upon double femtosecond pulse exposures, Appl. Surf. Sci. 336 (2014) 349–353.
[36] X. Jia, T.Q. Jia, Y. Zhang, P.X. Xiong, D.H. Feng, Z.R. Sun, J.R. Qiu, Z.Z. Xu, Periodic nanoripples in the surface and subsurface layers in ZnO irradiated by femtosecond laser pulses, Opt. Lett. 35 (2010) 1248–1250.
[37] C.S.R. Nathala, A. Ajami, A.A. Ionin, S.I. Kudryashov, S.V. Makarov, T. Ganz, A. Assion, W. Husinsky, Experimental study of fs-laser induced sub-100-nm periodic surface structures on titanium, Opt. Express 23 (2015) 5915–5929.
[38] T.C. Isabell, P.E. Fischione, C. O'Keefe, M.U. Guruz, V.P. Dravid, Plasma cleaning and its applications for electron microscopy, Microsc. Microanal. 5 (1999) 126–135.
[39] J.R. DeVore, Refractive indices of rutile and sphalerite, J. Opt. Soc. Am. 41 (1951) 416–419.
[40] Y.F. Zhao, T.J. Hou, Y.Y. Li, K.S. Chan, S.T. Lee, Effective increasing of optical absorption of TiO_2 by introducing trivalent titanium, Appl. Phys. Lett. 102 (2013) 171902.
[41] S. Kurian, H. Seo, H. Jeon, Significant enhancement in visible light absorption of TiO_2 nanotube arrays by surface band gap tuning, J. Phys. Chem. C 117 (2013) 16811–16819.